Philosophical Magazine

ISSN: 1478-6435 (Print) 1478-6443 (Online) Journal homepage: https://www.tandfonline.com/loi/tphm20

Atomic structure of γ" phase in Mg–Gd–Y–Ag alloy induced by Ag addition

Xuechao Sha, Lirong Xiao, Xuefei Chen, Guangming Cheng, Yandong Yu, Dongdi Yin & Hao Zhou

To cite this article: Xuechao Sha, Lirong Xiao, Xuefei Chen, Guangming Cheng, Yandong Yu, Dongdi Yin & Hao Zhou (2019): Atomic structure of γ″ phase in Mg–Gd–Y–Ag alloy induced by Ag addition, Philosophical Magazine, DOI: 10.1080/14786435.2019.1606466

To link to this article: https://doi.org/10.1080/14786435.2019.1606466

Published online: 14 Apr 2019.

PHILOSOPHICAL MAGAZINE
https://doi.org/10.1080/14786435.2019.1606466

Taylor & Francis
Taylor & Francis Group

Atomic structure of γ″ phase in Mg–Gd–Y–Ag alloy induced by Ag addition

Xuechao Sha[a], Lirong Xiao[a], Xuefei Chen[b,c], Guangming Cheng[d], Yandong Yu[e], Dongdi Yin[f] and Hao Zhou[b]

[a]Beijing Key Lab of Microstructure and Property of Advanced Materials, Beijing University of Technology, Beijing, People's Republic of China; [b]Nano and Heterogeneous Materials Center, School of Materials Science and Engineer, Nanjing University of Science and Technology, Nanjing, People's Republic of China; [c]State Key Laboratory of Nonlinear Mechanics, Institute of Mechanics, Chinese Academy of Sciences, Beijing, People's Republic of China; [d]Department of Mechanical and Aerospace Engineering, North Carolina State University, Raleigh, NC, USA; [e]School of Materials Science and Engineering, Harbin University of Science and Technology, Harbin, People's Republic of China; [f]Key Laboratory of Advanced Technologies of Materials, Ministry of Education, School of Materials Science and Engineering, Southwest Jiaotong University, Chengdu, Sichuan, People's Republic of China

ABSTRACT

Mg–Gd based alloys are typical high strength magnesium alloys owing to their outstanding age hardening behavior. The mechanical strength of aged Mg–Gd alloys is enhanced by high density prismatic-shaped precipitates in Mg matrix. Moreover, the addition of Ag has been found to enhance the strength of Mg–Gd based alloys further by forming a plate-shaped precipitate, named as γ″, on basal planes of Mg. However, the structure of this precipitate is not well understood due to the complex alloying system. In this work, the atomic structure of γ″ phase is investigated using atomic-resolution high-angle annular dark field scanning transmission electron microscopy (HAADF-STEM). Based on the accurate atomic structure from three independent directions, e.g. in $[0001]_{Mg}$, $[\bar{2}110]_{Mg}$ and $[01\bar{1}0]_{Mg}$ zone axes, the unit cell of γ″ is well established. The γ″ phase has a hexagonal structure, and its lattice parameters are $a = 0.55$ nm and $c = 0.42$ nm. The orientation relationship between γ″ phase and Mg matrix is $(0001)_{\gamma''}//(0001)_{Mg}$ and $<\bar{2}110>_{\gamma''}//<\bar{1}010>_{Mg}$.

ARTICLE HISTORY
Received 27 August 2018
Accepted 2 April 2019

KEYWORDS
Mg alloys; precipitation; HAADF-STEM; microstructural analysis

1. Introduction

Due to the low density and good castability, magnesium alloys show a promising prospect in the applications of light weighting and energy saving. However, relative low strength limits the application of magnesium alloys in industrial productions [1,2]. Hence, magnesium alloys containing a series of strengthening

CONTACT Lirong Xiao xiaolr620@126.com Beijing Key Lab of Microstructure and Property of Advanced Materials, Beijing University of Technology, Beijing 100124, People's Republic of China; Hao Zhou hzhou511@njust.edu.cn Nano and Heterogeneous Materials Center, School of Materials Science and Engineer, Nanjing University of Science and Technology, Nanjing 210094, People's Republic of China

elements have been developed. Among them, rare earth containing magnesium alloys (Mg-RE alloys), especially the Mg–Gd based alloys, are designed for their excellent age hardening effects [3–11]. For example, Li et al. [12] developed a Mg–14Gd alloy which obtained an ultimate tensile strength of 482 MPa after aging treatment. It has been well investigated that the high strength of Mg–Gd based alloys is mostly attributed to the β′ phase which is formed on prismatic planes of Mg matrix [13–15]. Nie et al. reported that the critical resolved shear stress (CRSS) increment induced by plate-shaped precipitates formed on prismatic planes of Mg matrix is significantly larger than other precipitations [16].

Based on the investigations of Mg–Gd binary alloys, the Mg–Gd–Y ternary alloys were developed for industrial applications. For one thing, the addition of yttrium was added to reduce the cost of raw materials effectively without sacrificing much precipitation strengthening [17]. It has been reported that a part of Gd atoms in β′ phase are replaced by Y atoms in Mg–Gd–Y alloys [18]. While, the price of Mg–Y master alloy is much lower than the Mg–Gd master alloy. For another, yttrium addition was reported to promote the non-basal slips in Mg alloys, which improve the formability of Mg significantly [19,20]. Therefore, extensive researches on Mg–Gd–Y alloys were carried out due to their excellent comprehensive performances [21–23].

Recent researches indicate that the addition of Ag can enhance the strength of Mg–Gd–Y alloys additionally [24–29]. Gao et al. [24] found that the hardness of Mg–6Gd–0.2Zr alloy was improved from 59 to 90 VHN by adding 2 wt.% of Ag. The increase of strength is affected by the extra basal plate precipitate coexisting with β′ phase. Such precipitations are consistent with the ideal precipitation microstructure in Mg–Gd based alloys, in which both the basal slip and non-basal slip of dislocations are effectively obstructed by precipitates [16,30,31]. It has been reported that the basal plate precipitate formed in Ag-containing Mg–Gd based alloy is similar to the γ″ phase formed in Mg–Gd–Zn alloys [32–36]. Different from the well-studied β′ phase, the structure of basal plate precipitate, especially its atomic structure, is still unclear. Saito et al. [35,36] proposed that the γ″ phase in Mg–Gd–Zn alloys is composed of Gd/Zn-enriched layer and Mg layer. While Nie et al. [33] believed that the γ″ phase is composed of Gd-enriched layer and Zn-enriched layer. The main reason for the controversy is that high resolution transmission electron microscopy (HRTEM) can only provide two-dimensional (2D) projection of the precipitates. However, it is difficult to obtain an accurate three-dimensional (3D) lattice structure with less than three projections from independent zone axes. In this work, the two Mg–Gd–Y alloys with similar compositions except for Ag containing were comparatively studied to explain the effect of Ag addition on precipitation behavior of Mg–Gd based alloy. The Gd and Ag are proven as the main alloying elements to form γ″ phase using energy-dispersive X-ray spectroscopy (EDS) mapping. Since the image intensity of the atomic columns is proportional to the square

of the atomic number Z [37], we were able to obtain *Z* contrast images to differentiate heavy solute atoms (Mg: 12, Gd: 64 and Ag: 47) in precipitates. The atomic positions of each atom in γ″ phase were identified by the atomic-resolution HAADF-STEM images viewed along $[0001]_{Mg}$, $[\bar{2}110]_{Mg}$ and $[01\bar{1}0]_{Mg}$ zone axes, respectively. The convincing 3D atomic structure of γ″ unit cell was established based on experimental and simulated results. In addition, the formation process of γ″ phase was discussed.

2. Materials and methods

Chemical compositions of the two alloys are Mg–8.5Gd–2.3Y (wt.%) except for 2 wt.% of Ag. The alloys were prepared from high purity Mg, Ag metals and Mg-25RE (wt.%) (RE = Y and Gd) master alloys in an electric resistant furnace under the mixed atmosphere of CO_2 and SF_6. The as-cast ingots were solution treated at 500°C for 12 h followed by quenching in hot water with 70°C. Isothermal ageing was performed at 200°C in silicon oil for 0–64 h. TEM samples were cut from the aged samples, then polished and dimpled to a thickness of ~30 μm. Ion milling was carried out using Precision Ion Polishing System (PIPS, Gatan model 695) at −25°C to avoid the damage on microstructure. The HAADF-STEM observation was performed on an FEI Titan G2 60–300 TEM with probe-spherical aberration at 300 kV. The atomic model was established using Crystal Maker software.

3. Results and discussion

Figure 1 shows the low magnification HAADF-STEM images of the Mg–Gd–Y and Mg–Gd–Y–Ag alloys aged at 200°C for 50 h. The brighter contrast in the images represent the heavier atom with a larger atomic number [37]. It is noticeable that the morphologies of the precipitations in the two alloys are different. Figure 1(a,b) shows the precipitates in Mg–Gd–Y alloy viewed from $[\bar{2}110]_{Mg}$ and $[0001]_{Mg}$ zone axes, respectively. The precipitates in Mg–Gd–Y alloy are elliptical shape when observed from $[0001]_{Mg}$ direction as shown in Figure 1 (b), which is the typical β′ phase in the Mg–Gd system alloys [38–41]. Interestingly, there are two kinds of precipitates in Mg–Gd–Y–Ag alloy aged in the same condition. Co-exiting with β′ phase, another precipitate which has horizontal strips parallel to the basal plane is observed in the matrix. The space between the horizontal strips is not a constant, which is larger than that of between the vertical strips (~1.1 nm) as shown in Figure 1(c). The morphology of the additional precipitate is same to the γ″ phase reported in Ref. [32–35, 42]. As shown in Figure 1(d), the morphology of this precipitate is in circle shape viewed from the $[0001]_{Mg}$ direction.

EDS mapping of Mg–Gd–Y–Ag alloy was performed in the region including both β′ and γ″ phases, as shown in Figure 2(a). It exhibits that the phases are

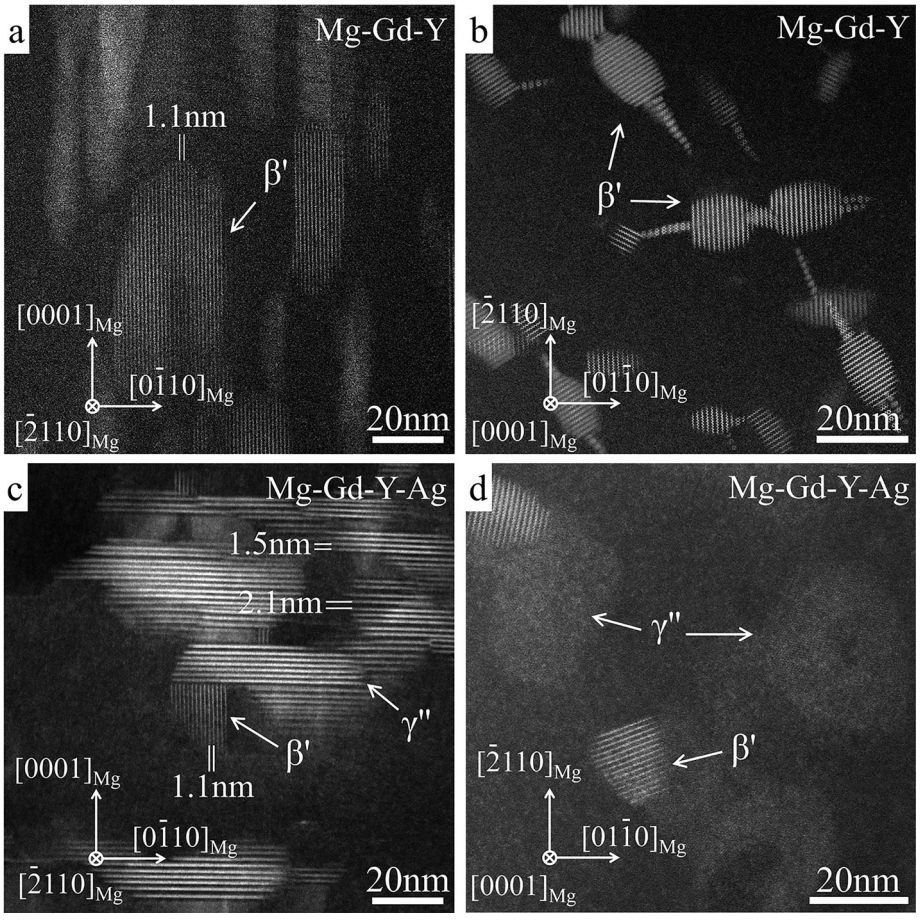

Figure 1. Low-magnified HAADF-STEM images of the samples aged at 200°C for 50 h: (a) and (b) the Mg–Gd–Y alloy viewed along $[\bar{2}110]_{Mg}$ and $[0001]_{Mg}$ zone axes; (c) and (d) the Mg–Gd–Y–Ag alloy viewed along $[\bar{2}110]_{Mg}$ and $[0001]_{Mg}$ zone axes, respectively.

mainly composed of Mg, Gd and Ag elements, while the Y is almost absent in the precipitates of Mg–Gd–Y–Ag alloy (see the Figure 2(b)–(d)). Similar results were found in the twin boundary segregation and interfacial phase of the same alloy [23,29]. The first principle calculation indicated that Ag has a negative energy value to form the precipitates in Mg–Gd–Y–Ag alloy, while the energies of Y and Zr are positive [23]. Owing to the easily precipitating of Ag, the tendency for precipitation of Y is negligible. Thus, only Gd, Ag and Mg will be considered in analyzing atomic occupation in this work.

Figure 3(a) shows the atomic-resolution HAADF-STEM image of γ″ phase viewed along $[0001]_{Mg}$ zone axis. This image is composed of the upper original part and bottom inverse Fourier-filtered (IFFT) part. Figure 3(b) shows the enlarged IFFT image of region A. As shown in Figure 3(b), there are three types of atomic columns which have different contrasts marked by orange,

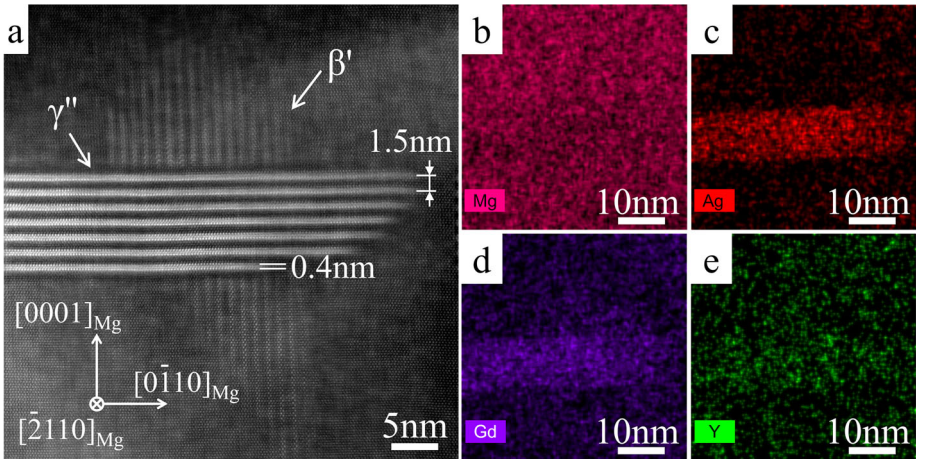

Figure 2. EDS chemical mapping of the β′ and γ″ phase in Mg–Gd–Y–Ag alloy: (a) the HAADF-STEM image, and the corresponding (b) Mg-Kα; (c) Ag-Kα; (d) Gd-Kα; and (e) Y-Kα distributions.

green and blue colors, respectively. Figure 3(c) and (d) show the integrating intensity of column brightness obtained from regions I and II. The atomic columns with the weakest brightness (marked by the blue points) have an intensity of $\sim 4 \times 10^2$, which is close to the α-Mg columns in the matrix. It is used as a benchmark brightness to investigate other segregated atomic columns comparatively. Clearly, the other two kinds of columns in this zone axis marked by green and orange points are much brighter, which show intensities of $\sim 7 \times 10^2$ and $\sim 13 \times 10^2$, respectively. According to Equation (1), the intensity of atomic

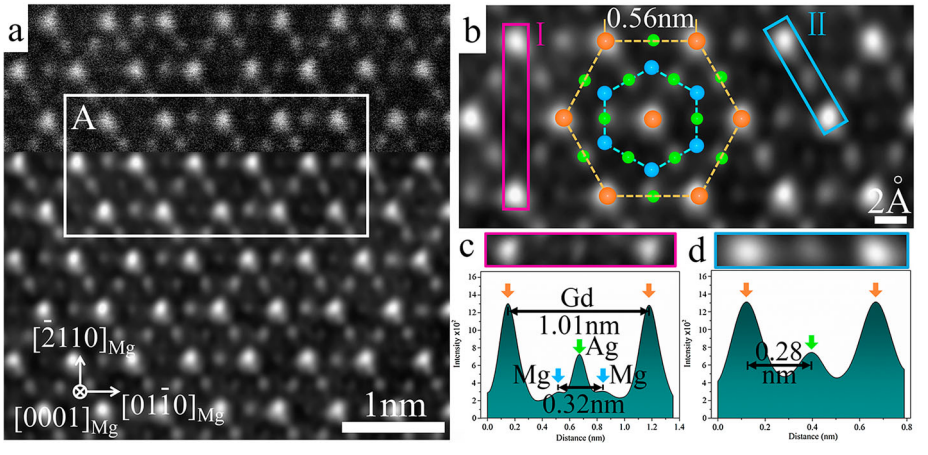

Figure 3. (a) The atomic-resolution HAADF-STEM image of γ″ phase, viewed along $[0001]_{Mg}$ zone axis. The upper part is the original HAADF image, and the bottom part is the IFFT image; (b) enlarged image of the region A; (c) and (d) brightness analysis of atomic columns implemented from the regions I and II.

columns in a HAADF image is approximately proportional to the square of atomic number Z [43].

$$\sigma_{(\theta)} = \frac{e^4 Z^2 \mathrm{d}\Omega}{16(4\pi\varepsilon_0 E_0)^2 \sin^4 \frac{\theta}{2}}, \quad (1)$$

pwhere σ is scattering cross section, θ is scattering semi-angle, Ω is the solid angle, e is electron charge, Z is an atomic number, ε_0 is the dielectric constant and E_0 is the energy of the electrons.

Based on this equation, the intensity brightness indicates that the other two columns marked by orange and green points are Gd and Ag enriched columns, respectively. Figure 3(c) shows that the Gd and Mg enriched columns are symmetrical to an Ag column, and the distances between two Gd columns and two Mg columns along $<\bar{2}110>_{Mg}$ direction are ~1.01 and ~ 0.32 nm, respectively. As shown in Figure 3(b), two concentric hexagons are observed, which have Gd and Mg columns at the apexes of hexagon, respectively. The side length of the bigger hexagon is ~0.56 nm, which has the Ag columns at the midpoint of each side. Similarly, the smaller hexagon exhibits the same structure, which also has Ag columns at the midpoint of each side. The side length of the smaller hexagon is ~0.32 nm.

Figure 4(a) shows the HAADF-STEM image of γ″ phase viewed along $[\bar{2}110]_{Mg}$ zone axis, which is composed of a right original part and a left IFFT parts. There are four γ″ phases in the observed region, which exhibit strip-shape morphology parallel to the $<0\bar{1}10>_{Mg}$ direction. There are three adjacent layers in each γ″ phase, which have much brighter contrast than the Mg matrix.

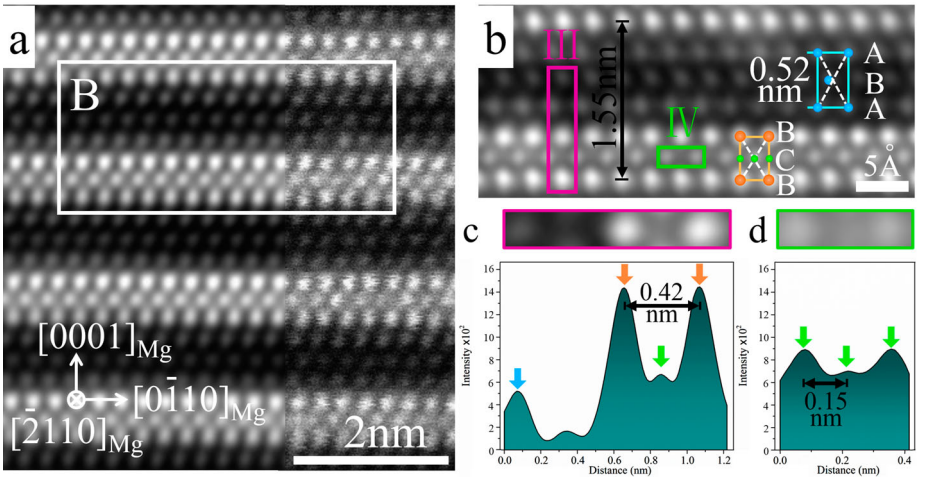

Figure 4. (a) The atomic-resolution HAADF-STEM image of γ″ phase, viewed along $[\bar{2}110]_{Mg}$ zone axis. The right part is the original HAADF image, and the rest is the IFFT image; (b) enlarged image of the region B; (c) and (d) the brightness analysis of atomic columns implemented from the regions III and IV.

The γ″ phases are alternately stacked with layers of Mg matrix along <0001>$_{Mg}$ direction. Most of them have three Mg layers as shown in Figure 4(a). Figure 4 (b) shows an enlarged IFFT image of region B. It is found that the stacking sequence of atomic layers in γ″ phase is BCB, which is different from the … ABAB … stacking sequence of Mg matrix.

Figure 4(c,d) shows the integrating intensity of column brightness obtained from regions III and IV. As shown in Figure 4(c), the brightness morphology of γ″ phase like a sandwich, which has two brightest atomic layers on the top and bottom, and a weaker layer in the middle. The brightness of Mg column in the matrix is weaker than the columns in γ″ phase. Hence, the middle layer of γ″ phase is probably composed of Ag enriched columns, and the two brightest layers on the top and bottom are proposed to be Gd-enriched columns. The spacing between the two Gd layers is ~0.42 nm, which is smaller than the length of *c* (0.52 nm) in Mg matrix. The spacing of Mg columns in the same layer is two times as the spacing of Ag columns (~0.15 nm).

Figure 5(a) shows the atomic-resolution HAADF-STEM image of γ″ phase viewed along $[01\bar{1}0]_{Mg}$ zone axis. Also, the right part is the original HAADF image, and the left one is the IFFT image. The morphology of γ″ observed along this direction is similar to that of $[\bar{2}110]_{Mg}$ direction, exhibiting the strip-shape parallel to basal planes of Mg matrix. This morphology indicates that γ″ phase in Mg–Gd–Y–Ag alloy is a basal plate precipitate, and has only three atomic layers thicknesses in the $[0001]_{Mg}$ direction. Figure 5(b) is the enlarged image of region C. The atomic columns with different brightness are also marked by the orange, green and blue colors, respectively. Note that, the top and bottom layers in γ″ phase are not composed of Gd columns. There are two Mg columns between each Gd column in the same layer. Figure 5(c,

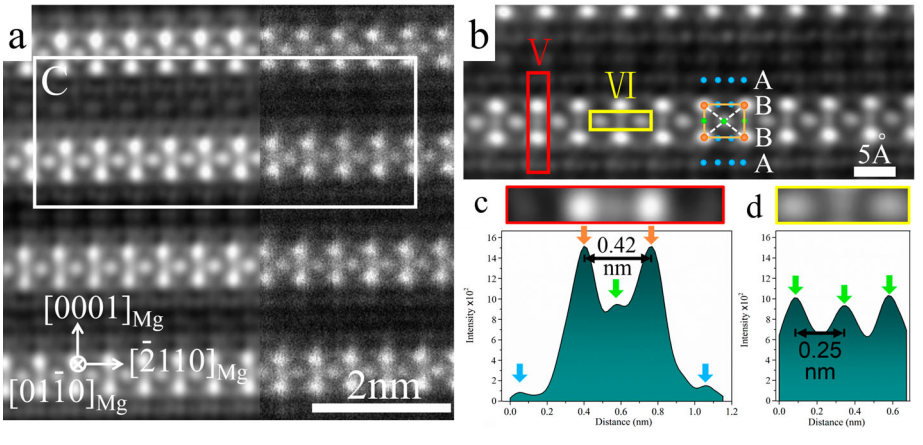

Figure 5. (a) The atomic-resolution HAADF-STEM image of γ″ phase, viewed along $[01\bar{1}0]_{Mg}$ zone axis. The right part is the original HAADF image, and the rest is the IFFT image; (b) enlarged image of the region C; (c) and (d) the brightness analysis of atomic columns implemented from the regions V and VI.

d) show the integrating intensity of column brightness obtained from regions V and VI. The distance between Ag columns in the middle layer is ~0.25 nm, which is larger than the space of Ag columns viewed from $[\bar{2}110]_{Mg}$ zone axis (Figure 4).

Figure 6 shows the selected area diffraction pattern (SADP) and corresponding simulated patterns in $[0001]_{Mg}$ zone axis. The simulated diffraction patterns (Figure 6(b,c)) indicate that the SADP in Figure 6(a) is mixed by pure Mg and γ″ phase. Owing to the high intensity of Mg matrix, the spots of $\{1\bar{1}00\}_{Mg}$ are very bright. It reveals that the spots of $\{1\bar{2}10\}_{\gamma''}$ are overlapped with the spots of $\{1\bar{1}00\}_{Mg}$. The interplanar spacing of $(1\bar{2}10)_{\gamma''}$ and $(1\bar{1}00)_{\gamma''}$ obtained from the SADP diffraction patterns are 0.274 and 0.470 nm, respectively. Based on the above analysis, the crystal structure of γ″ phase is determined as a hexagonal structure. The HAADF-STEM images in Figures 4 and 5 indicate that the γ″ phase is a basal plate precipitate with only three basal layers. It is hard to obtain a clear SADP in $[11\bar{2}0]$ or $[10\bar{1}0]$ zone axes due to the ultra-thin lamellar structure of γ″ phase. The *c*-axis length of γ″ phase is measured by the HAADF-STEM images in Figures 4 and 5, which shows an interplanar spacing of $(0001)_{\gamma''}$ of ~0.21 nm.

According to the atomic positions in γ″ phase shown in the above analysis, the 3D unit cell model of γ″ is established as shown in Figure 7(a). The orange, green and blue spheres represent Gd, Ag and Mg atoms, respectively. It shows that the γ″ phase has a hexagonal crystal structure, with a space group of *P6/mmm*. The lattice parameters of γ″ phase are $a = 0.55$ nm and $c = 0.42$ nm. The orientation relationship between γ″ phase and Mg matrix is $(0001)_{\gamma''}//(0001)_{Mg}$ and $<\bar{2}110>_{\gamma''}//<\bar{1}010>_{Mg}$. Total atom number in the unit cell is six, and the ratio of Mg, Gd and Ag is 2:1:3. The composition of γ″ phase obtained from the model is $Mg_2Gd_1Ag_3$. Figure 7(b)–(d) show the model of γ″ phase and corresponding IFFT images viewed along $[0001]_{Mg}$, $[\bar{2}110]_{Mg}$ and $[01\bar{1}0]_{Mg}$, respectively. The model exhibits a good match with the HAADF-STEM images. As shown in Figure 7(c,d), the Ag columns marked by green and red arrows have different brightness. It is because that

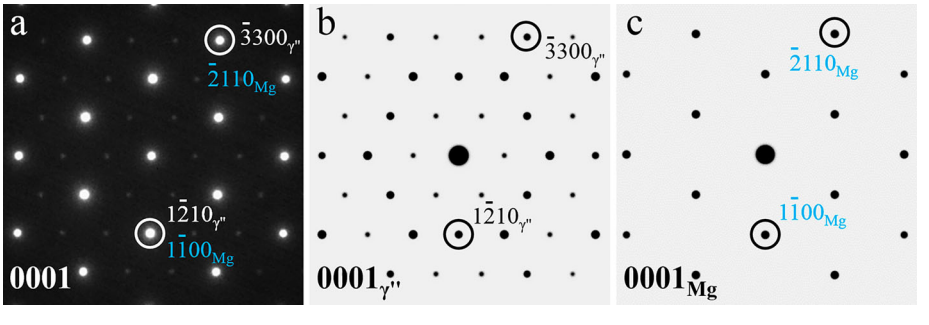

Figure 6. (a) The SADP of γ″ phase viewed from $[0001]_{Mg}$ zone axis, (b) and (c) corresponding simulated diffraction patterns of γ″ phase and pure Mg in $[0001]_{Mg}$ zone axis, respectively.

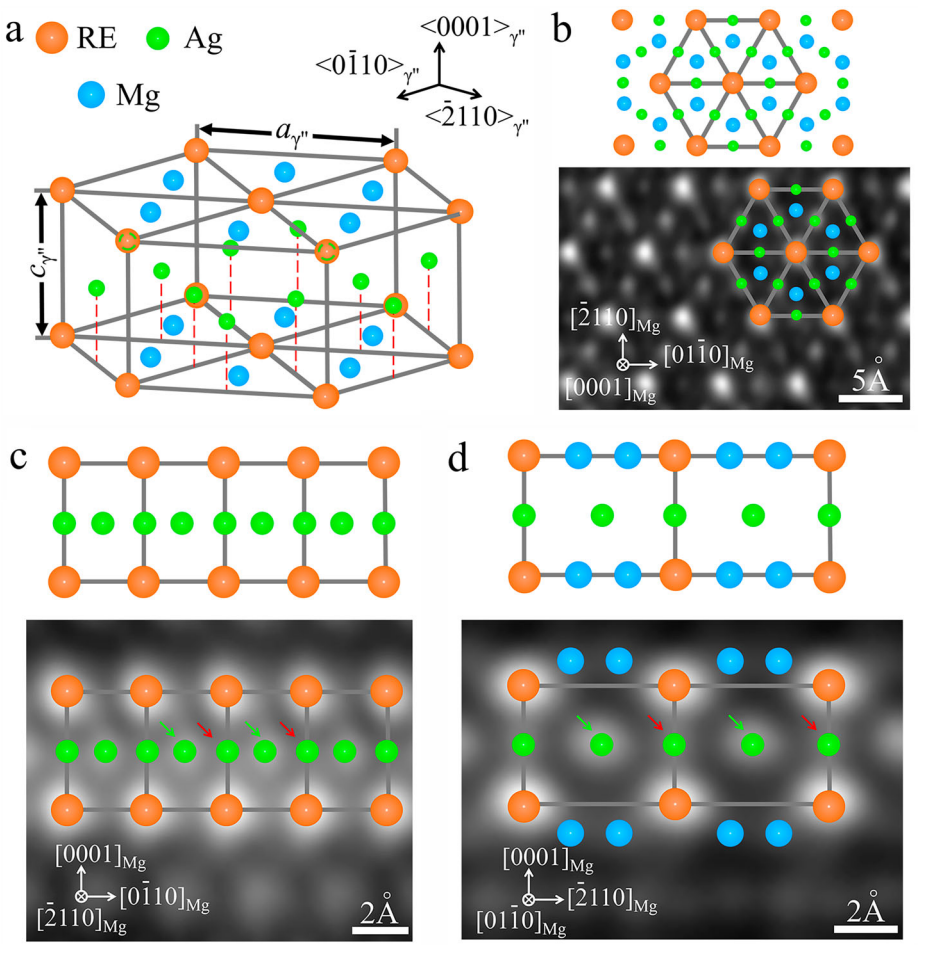

Figure 7. (a) The 3D atomic model of the unit cell of γ″ phase; (b)–(d) the model of γ″ phase and corresponding IFFT images viewed along $[0001]_{Mg}$, $[\bar{2}110]_{Mg}$ and $[01\bar{1}0]_{Mg}$, respectively.

the atomic spacing in the two columns is different, which results to different number of Ag atoms in these columns.

Note that, the models of γ″ phase were controversial in previous works. Two different lattice structure have been proposed in different works [42,44]. The main reason for this controversy is both of them had insufficient experimental data from only two zone axes, i.e. the <11$\bar{2}$0> and <10$\bar{1}$0> zone axes. Both of the two zone axes are parallel to the basal plane of Mg matrix. Therefore, the researchers had to speculate the atomic occupation of alloying elements in (0001) plane. In this work, the structure of γ″ phase is convinced by HAADF-STEM images from three independent zone axes, which provides solid evidence for structure determination. The SADP result also exhibits a good agreement with the simulated pattern of crystal model as shown in Figure 6.

In addition, the microstructure of γ″ phase in Mg–Gd–Y–Ag alloy is greatly different from the LPSO phase reported in Zn containing Mg alloys [31,44,45].

The LPSO phases have ABC stacking in some layers of basal planes, which induce local FCC stacking in the HCP structural Mg matrix. However, the crystal structure of γ″ phase in Mg–Gd–Y–Ag alloy is still an HCP structure. While the orientation of crystal structure is rotated for 30 degrees along *c*-axis of the Mg matrix as revealed in the SADP analysis in Figure 6.

4. Conclusions

The γ″ phase, which is induced by Ag, co-exists with β′ phase in Mg–Gd–Y–Ag alloy. The Gd and Ag are proven as the main alloying elements of both the β′ and γ″ phases. The atomic structure of the γ″ phase in Mg–Gd–Y–Ag alloy has been investigated using atomic-resolution HAADF-STEM imaging viewed from three independent directions. The accurate atomic model of γ″ phase is determined as a hexagonal structure, which has lattice parameters of $a = 0.55$ nm and $c = 0.42$ nm. The orientation relationship between γ″ phase and Mg matrix is $(0001)_{\gamma''}//(0001)_{Mg}$ and $<\bar{2}110>_{\gamma''}//<\bar{1}010>_{Mg}$.

Disclosure statement

No potential conflict of interest was reported by the authors.

Funding

This work was supported by the National Key Research and Development Program of China [grant numbers 2017YFA0204403, 2017YFB0305501]; National Natural Science Foundation of China [grant numbers 51601003, 51401172, 51074106, 51374145]; Natural Science Foundation of Heilongjiang Province [grant number QC2017061]; Harbin Science and Technology Bureau [grant number 2017RAQXJ066].

References

[1] B.L. Mordike and T. Ebert, *Magnesium properties-applications-potential*. Mater. Sci. Eng. A 302 (2001), pp. 37–45.
[2] I.J. Polmear, *Magnesium alloys and applications*. Mater. Sci. Technol. 10 (1994), pp. 1–16.
[3] J.F. Nie, X. Gao, and S.M. Zhu, *Enhanced age hardening response and creep resistance of Mg-Gd alloys containing Zn*. Scr. Mater. 53 (2005), pp. 1049–1053.
[4] J.D. Robson, N. Stanford, and M.R. Barnett, *Effect of precipitate shape on slip and twinning in magnesium alloys*. Acta Mater. 59 (2011), pp. 1945–1956.
[5] W. Guo, Q.D. Wang, B. Ye, M.P. Liu, T. Peng, X.T. Liu, and H. Zhou, *Enhanced microstructure homogeneity and mechanical properties of AZ31 magnesium alloy by repetitive upsetting*. Mater. Sci. Eng. A 540 (2012), pp. 115–122.
[6] H. Zhou, Q.D. Wang, B. Ye, and W. Guo, *Hot deformation and processing maps of as-extruded Mg-9.8Gd-2.7Y-0.4Zr Mg alloy*. Mater. Sci. Eng. A 576 (2013), pp. 101–107.

[7] L. Zhang, B. Ye, W.J. Liao, H. Zhou, W. Guo, Q.D. Wang, H.Y. Jiang, and W.J. Ding, *Microstructure evolution and mechanical properties of AZ91D magnesium alloy processed by repetitive upsetting*. Mater. Sci. Eng. A 641 (2015), pp. 62–70.
[8] J.X. Zheng, Z. Li, L.D. Tan, X.S. Xu, R.C. Luo, and B. Chen, *Precipitation in Mg-Gd-Y-Zr alloy: atomic-scale insights into structures and transformations*. Mater. Charact. 117 (2016), pp. 76–83.
[9] W. Rong, Y. Zhang, Y.J. Wu, Y.L. Chen, T. Tang, L.M. Peng, and D.Y. Li, *Fabrication of high-strength Mg-Gd-Zn-Zr alloys via differential-thermal extrusion*. Mater. Charact. 131 (2017), pp. 380–387.
[10] Y.M. Zhu, M.Z. Bian, and J.F. Nie, *Tilt boundaries and associated solute segregation in a Mg-Gd alloy*. Acta Mater. 127 (2017), pp. 505–518.
[11] W.T. Sun, X.G. Qiao, M.Y. Zheng, C. Xu, S. Kamado, X.J. Zhao, H.W. Chen, N. Gao, and M.J. Starink, *Altered ageing behaviour of a nanostructured Mg-8.2Gd-3.8Y-1.0Zn-0.4Zr alloy processed by high pressure torsion*. Acta Mater. 151 (2018), pp. 260–270.
[12] R.G. Li, J.F. Nie, G.J. Huang, Y.C. Xin, and Q. Liu, *Development of high-strength magnesium alloys via combined processes of extrusion, rolling and ageing*. Scr. Mater. 64 (2011), pp. 950–953.
[13] S.M. He, X.Q. Zeng, L.M. Peng, X. Gao, J.F. Nie, and W.J. Ding, *Microstructure and strengthening mechanism of high strength Mg-10Gd-2Y-0.5Zr alloy*. J. Alloys Compd. 427 (2007), pp. 316–323.
[14] K. Yamada, H. Hoshikawa, S. Maki, T. Ozaki, Y. Kuroki, S. Kamado, and Y. Kojima, *Enhanced age-hardening and formation of plate precipitates in Mg-Gd-Ag alloys*. Scr. Mater. 61 (2009), pp. 636–639.
[15] Y. Zhang, Y.J. Wu, L.M. Peng, P.H. Fu, F. Huang, and W.J. Ding, *Microstructure evolution and mechanical properties of an ultra-high strength casting Mg-15.6 Gd-1.8 Ag-0.4 Zr alloy*. J. Alloys Compd. 615 (2014), pp. 703–711.
[16] J.F. Nie, *Effects of precipitate shape and orientation on dispersion strengthening in magnesium alloys*. Scr. Mater. 48 (2003), pp. 1009–1015.
[17] L.L. Rokhlin and N.I. Nikitina, *Magnesium-Gadolinium and magnesium-Gadolinium-yttrium alloys*. Z. Metallkd 85 (1994), pp. 819–823.
[18] T. Honma, T. Ohkubo, K. Hono, and S. Kamado, *Chemistry of nanoscale precipitates in Mg-2.1Gd-0.6Y-0.2Zr (at.%) alloy investigated by the atom probe technique*. Mater. Sci. Eng. A 395 (2005), pp. 301–306.
[19] Z.G. Ding, W. Liu, H. Sun, S. Li, D.L. Zhang, Y.H. Zhao, E.J. Lavernia, and Y.T. Zhu, *Origins and dissociation of pyramida <c+a> dislocations in magnesium and its alloys*. Acta Mater. 146 (2018), pp. 265–272.
[20] Z. Wu, R. Ahmad, B. Yin, S. Sandlöbes, and W.A. Curtin, *Mechanistic origin and prediction of enhanced ductility in magnesium alloys*. Science 359 (2018), pp. 447–452.
[21] T. Homma, N. Kunito, and S. Kamado, *Fabrication of extraordinary high-strength magnesium alloy by hot extrusion*. Scr. Mater. 61 (2009), pp. 644–647.
[22] W.T. Sun, X.G. Qiao, M.Y. Zheng, X.J. Zhao, H.W. Chen, N. Gao, and M.J. Starink, *Achieving ultra-high hardness of nanostructured Mg-8.2Gd-3.2Y-1.0Zn-0.4Zr alloy produced by a combination of high pressure torsion and ageing treatment*. Scr. Mater. 155 (2018), pp. 21–25.
[23] L.R. Xiao, Y. Cao, S. Li, H. Zhou, X.L. Ma, L. Mao, X.C. Sha, Q.D. Wang, Y.T. Zhu, and X.D. Han, *The formation mechanism of a novel interfacial phase with high thermal stability in a Mg-Gd-Y-Ag-Zr alloy*. Acta Mater. 162 (2019), pp. 214–225.
[24] X. Gao and J.F. Nie, *Enhanced precipitation-hardening in Mg-Gd alloys containing Ag and Zn*. Scr. Mater. 58 (2008), pp. 619–622.

[25] Q.D. Wang, J. Chen, Z. Zhao, and S.M. He, *Microstructure and super high strength of cast Mg-8.5Gd-2.3Y-1.8Ag-0.4Zr alloy*. Mater. Sci. Eng. A 528 (2010), pp. 323–328.
[26] H. Zhou, Q.D. WANG, J. Chen, B. Ye, and W. Guo, *Microstructure and mechanical properties of extruded Mg-8.5 Gd-2.3 Y-1.8 Ag-0.4 Zr alloy*. Trans. Nonferrous Met. Soc. China 22 (2012), pp. 1891–1895.
[27] J. Feng, H.F. Sun, X.W. Li, H. Wang, and W.B. Fang, *Effects of Ag variations on dynamic recrystallization, texture, and mechanical properties of ultrafine-grained Mg-3Al-1Zn alloys*. J. Mater. Res. 31 (2016), pp. 3360–3371.
[28] Y. Zhang, W. Rong, Y.J. Wu, L.M. Peng, J.F. Nie, and N. Birbilis, *A comparative study of the role of Ag in microstructures and mechanical properties of Mg-Gd and Mg-Y alloys*. Mater. Sci. Eng. A 731 (2018), pp. 609–622.
[29] H. Zhou, G.M. Cheng, X.L. Ma, W.Z. Xu, S.N. Mathaudhu, Q.D. Wang, and Y.T. Zhu, *Effect of Ag on interfacial segregation in Mg-Gd-Y-(Ag)-Zr alloy*. Acta Mater. 95 (2015), pp. 20–29.
[30] S.M. He, X.Q. Zeng, L.M. Peng, X. Gao, J.F. Nie, and W.J. Ding, *Precipitation in a Mg-10Gd-3Y-0.4Zr (wt.%) alloy during isothermal ageing at 250°C*. J. Alloys Compd. 421 (2006), pp. 309–313.
[31] J.F. Nie, *Precipitation and hardening in magnesium alloys*. Metall. Mater. Trans. A 43 (2012), pp. 3891–3939.
[32] M. Nishijima, K. Hiraga, M. Yamasaki, and Y. Kawamura, *The structure of Guinier-Preston Zones in an Mg-2 at%Gd-1 at%Zn alloy studied by transmission electron microscopy*. Mater. Trans. 49 (2008), pp. 227–229.
[33] J.F. Nie, K. Oh-ishi, X. Gao, and K. Hono, *Solute segregation and precipitation in a creep-resistant Mg-Gd-Zn alloy*. Acta Mater. 56 (2008), pp. 6061–6076.
[34] Y.M. Zhu, A.J. Morton, and J.F. Nie, *Characterisation of intermetallic phases in an Mg-Y-Ag-Zn casting alloy*. Phil. Mag. Lett. 90 (2010), pp. 173–181.
[35] K. Saito, M. Nishijima, and K. Hiraga, *Stabilization of Guinier-Preston zones in hexagonal close-packed Mg-Gd-Zn alloys studied by transmission electron microscopy*. Mater. Trans. 51 (2010), pp. 1712–1714.
[36] K. Saito, A. Yasuhara, and K. Hiraga, *Microstructural changes of Guinier-Preston zones in an Mg-1.5 at%Gd-1at%Zn alloy studied by HAADF-STEM technique*. J. Alloys Compd. 509 (2011), pp. 2031–2038.
[37] J.F. Nie, Y.M. Zhu, J.Z. Liu, and X.Y. Fang, *Periodic segregation of solute atoms in fully coherent twin boundaries*. Science 340 (2013), pp. 957–960.
[38] M. Nishijima and K. Hiraga, *Structural changes of precipitates in an Mg-5at%Gd alloy studied by transmission electron microscopy*. Mater. Trans. 48 (2007), pp. 10–15.
[39] M. Nishijima, K. Hiraga, M. Yamasaki, and Y. Kawamura, *Characterization of β′ phase precipitates in an Mg-5at%Gd alloy aged in a peak hardness condition, studied by high-angle annular detector dark-field scanning transmission electron microscopy*. Mater. Trans. 47 (2006), pp. 2109–2112.
[40] X. Gao, S.M. He, X.Q. Zeng, L.M. Peng, W.J. Ding, and J.F. Nie, *Microstructure evolution in a Mg-15Gd-0.5Zr (wt.%) alloy during isothermal aging at 250°C*. Mater. Sci. Eng. A 431 (2006), pp. 322–327.
[41] H. Zhou, W.Z. Xu, W.W. Jian, G.M. Cheng, X.L. Ma, W. Guo, S.N. Mathaudhu, Q.D. Wang, and Y.T. Zhu, *A new metastable precipitate phase in Mg-Gd-Y-Zr alloy*. Phil. Mag. 94 (2014), pp. 2403–2409.
[42] Z. Li, J.X. Zheng, and B. Chen, *Unravelling the structure of γ″ in Mg-Gd-Zn: an atomic-scale HAADF-STEM investigation*. Mater. Charact. 120 (2016), pp. 345–348.
[43] D.B. Williams and C.B. Carter, *Transmission Electron Microscopy: A Textbook for Materials Science*, 2nd ed., Springer, Boston, 2009, pp. 760.

[44] Y.M. Zhu, K. Oh-ishi, N.C. Wilson, K. Hono, A.J. Morton, and J.F. Nie, *Precipitation in a Ag-containing Mg-Y-Zn alloy*. Mater. Sci. Eng. A 47 (2016), pp. 927–940.
[45] Y.M. Zhu, A.J. Morton, and J.F. Nie, *The 18R and 14H long-period stacking ordered structures in Mg-Y-Zn alloys*. Acta Mater. 58 (2010), pp. 2936–2947.